

AperTO - Archivio Istituzionale Open Access dell'Università di Torino

Assessing the photodegradation potential of compounds derived from the photoinduced weathering of polystyrene in water

This is a pre print version of the following article:

Original Citation:

Availability:

This version is available <http://hdl.handle.net/2318/1900593> since 2023-06-04T14:00:42Z

Published version:

DOI:10.1016/j.scitotenv.2023.162729

Terms of use:

Open Access

Anyone can freely access the full text of works made available as "Open Access". Works made available under a Creative Commons license can be used according to the terms and conditions of said license. Use of all other works requires consent of the right holder (author or publisher) if not exempted from copyright protection by the applicable law.

(Article begins on next page)

Chemosphere

Assessing the photodegradation potential of compounds derived from the photoinduced weathering of polystyrene in water

--Manuscript Draft--

Manuscript Number:	
Article Type:	Research paper
Section/Category:	Environmental Chemistry
Keywords:	Environmental photochemistry; Photochemical fate; Kinetic constant; Polystyrene; Aromatic compounds; Natural waters
Corresponding Author:	Davide Vione University of Turin: Universita degli Studi di Torino Torino, ITALY
First Author:	Debora Fabbri
Order of Authors:	Debora Fabbri Luca Carena Debora Bertone Marcello Brigante Monica Passananti Davide Vione
Abstract:	<p>Benzoate (Bz⁻) and acetophenone (AcPh) are aromatic compounds known to be produced by sunlight irradiation of polystyrene aqueous suspensions. Here we show that these molecules could react with •OH (Bz⁻) and •OH + CO₃^{•-} (AcPh) in sunlit natural waters, while other photochemical processes (direct photolysis and reaction with singlet oxygen, or with the excited triplet states of chromophoric dissolved organic matter) are unlikely to be important. In the case of AcPh, a competitive process to aqueous-phase photodegradation could be volatilisation followed by reaction with gas-phase •OH. As far as Bz⁻ is concerned, elevated DOC levels could be important in protecting this compound from aqueous-phase photodegradation. Limited reactivity of the studied compounds with the dibromine radical (Br₂^{•-}) suggests that •OH scavenging by bromide, which yields Br₂^{•-}, would be poorly offset by Br₂^{•-}-induced degradation. Therefore, photodegradation kinetics of Bz⁻ and AcPh should be slower in seawater (containing [Br⁻] ~ 1 mM) compared to freshwaters. The present findings suggest that photochemistry would play a role both in the formation of water-soluble organic compounds upon weathering of plastic particles, and in their degradation.</p>
Suggested Reviewers:	Weihua Song Fudan University wsong@fudan.edu.cn Marcela P Silva São Paulo State University marcela.prado@unesp.br Steven Loiselle University of Siena steven.loiselle@unisi.it Carsten Prasse Johns Hopkins University cprasse1@jhu.edu Cecilia Arsene Faculty of Chemistry Alexandru Ioan Cuza University carsene@uaic.ro Hansun Fang

	Jiangxi Agricultural University fanghansun@163.com
Opposed Reviewers:	



UNIVERSITÀ DEGLI STUDI DI TORINO

DIPARTIMENTO DI CHIMICA

Via P. Giuria,5 - 10125 TORINO (ITALY)

Tel. 011/6705296 Fax 011/6705242

Codice Fiscale 80088230018 - Partita IVA 02099550010

Chemosphere Editorial Office

Torino, 16 December 2022

Dear Sir/Madam,

I am pleased to submit the manuscript entitled “**Assessing the photodegradation potential of compounds derived from the photoinduced weathering of polystyrene in water**” by Debora Fabbri, Debora Bertone, Luca Carena, Marcello Brigante, Monica Passananti, and Davide Vione, for consideration by *Chemosphere*.

Pollution by plastics is an important environmental problem, due to the plastic load to the environment. Furthermore, plastics weathering is a known source of chemical compounds for, most notably, surface waters. Compounds released by plastics could in turn undergo degradation, but comparatively little is known over this latter issue.

In this paper we investigate the photochemical degradation of benzoate and acetophenone, which are both released by polystyrene particles when exposed to sunlight, under conditions that are representative of sunlit surface waters. We also model two possible environmental scenarios: in the former, benzoate forms from polystyrene particles floating at the water surface and undergoes photodegradation in the aqueous phase; in the latter scenario, acetophenone undergoes both aqueous-phase photodegradation and volatilisation to the gas phase, where it is degraded by $\bullet\text{OH}$.

The current findings will contribute to the elucidation and better understanding of the environmental behaviour of compounds released by plastic particles.

We also declare that this study does not involve human subjects.

Sincerely,

A handwritten signature in blue ink that reads 'Davide Vione'.

Davide Vione

Debora Fabbri: Investigation; Validation; Formal analysis; Data curation; Writing - original draft.

Luca Carena: Investigation; Formal analysis; Data curation; Writing - original draft; Writing - review & editing.

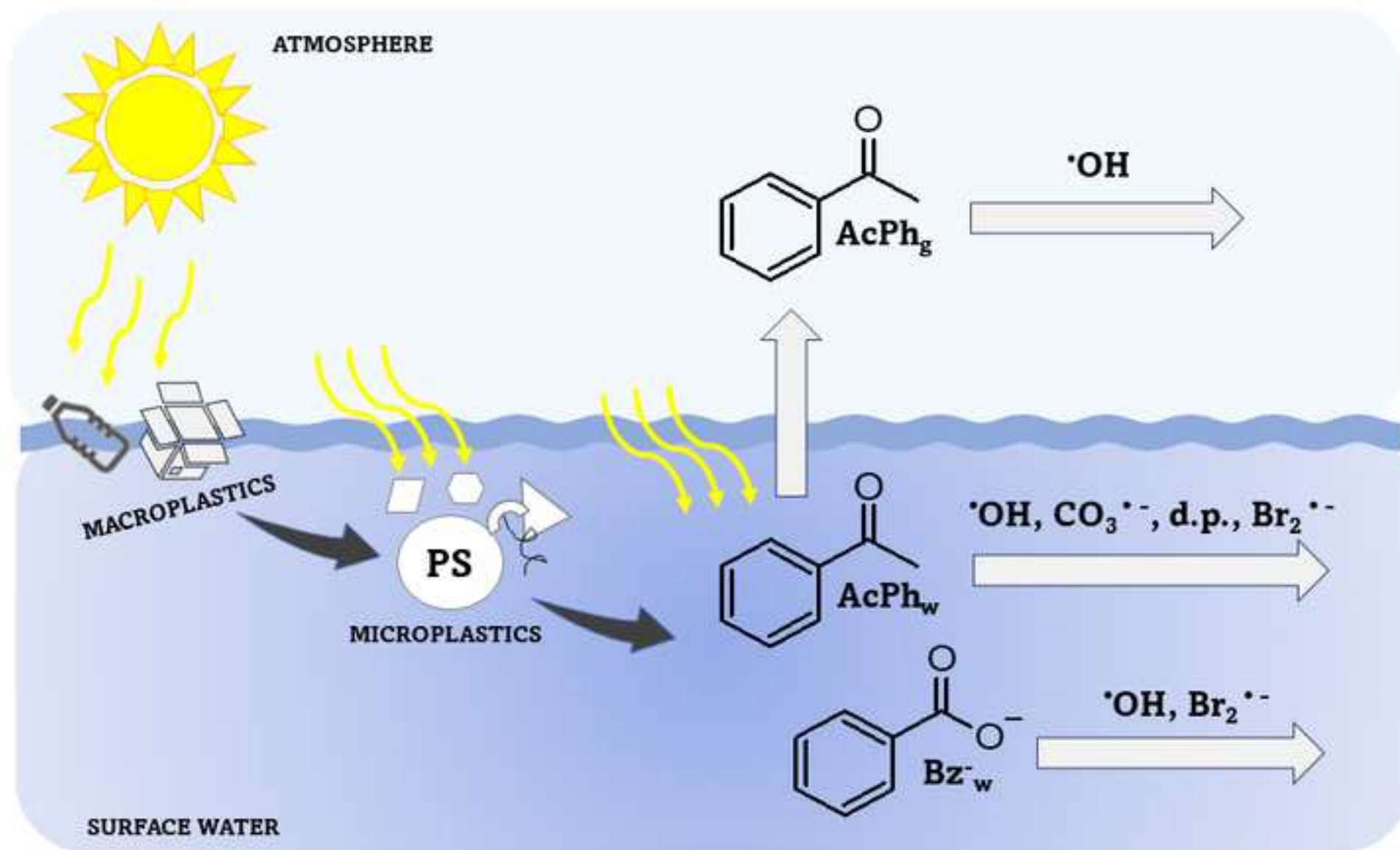
Debora Bertone: : Investigation; Data curation; Writing - original draft.

Marcello Brigante: Investigation; Validation; Data curation; Writing - review & editing.

Monica Passananti: Funding acquisition; Conceptualization; Writing - review & editing.

Davide Vione: Conceptualization; Investigation; Supervision; Validation; Data curation; Writing - original draft; Writing - review & editing.

- Both benzoate and acetophenone undergo important reactions with $\bullet\text{OH}$
- Acetophenone is also degraded by $\text{CO}_3^{\bullet-}$, while its direct photolysis would be minor
- Volatilisation would be an important removal pathway for aqueous acetophenone
- Both compounds show limited reactivity with $\text{Br}_2^{\bullet-}$
- Both compounds have higher stability in high-DOC freshwaters and in seawater



Declaration of interests

The authors declare that they have no known competing financial interests or personal relationships that could have appeared to influence the work reported in this paper.

The authors declare the following financial interests/personal relationships which may be considered as potential competing interests:

1 **Assessing the photodegradation potential of compounds derived from the**
2 **photoinduced weathering of polystyrene in water**

3

4 **Debora Fabbri,^a Luca Carena,^a Debora Bertone,^a Marcello Brigante,^b Monica Passananti,^{a,c,*}**

5 **Davide Vione^{a,*}**

6

7 *^a Dipartimento di Chimica, Università di Torino, Via Pietro Giuria 5, 10125 Torino, Italy*

8 *^b Université Clermont Auvergne, CNRS, INP Clermont Auvergne, Institut de Chimie de Clermont-*
9 *Ferrand, F-63000 Clermont-Ferrand, France*

10 *^c Institute for Atmospheric and Earth System Research/Physics, Faculty of Science, University of*
11 *Helsinki, FI-00014 Helsinki, Finland*

12

13 * Address correspondence to either author: monica.passananti@helsinki.fi (MP),

14 davide.vione@unito.it (DV)

15

16 ***Abstract***

17

18 Benzoate (Bz⁻) and acetophenone (AcPh) are aromatic compounds known to be produced by
19 sunlight irradiation of polystyrene aqueous suspensions. Here we show that these molecules could
20 react with •OH (Bz⁻) and •OH + CO₃^{•-} (AcPh) in sunlit natural waters, while other photochemical
21 processes (direct photolysis and reaction with singlet oxygen, or with the excited triplet states of
22 chromophoric dissolved organic matter) are unlikely to be important. In the case of AcPh, a
23 competitive process to aqueous-phase photodegradation could be volatilisation followed by reaction
24 with gas-phase •OH. As far as Bz⁻ is concerned, elevated DOC levels could be important in
25 protecting this compound from aqueous-phase photodegradation. Limited reactivity of the studied

26 compounds with the dibromine radical ($\text{Br}_2^{\bullet-}$) suggests that $\bullet\text{OH}$ scavenging by bromide, which
27 yields $\text{Br}_2^{\bullet-}$, would be poorly offset by $\text{Br}_2^{\bullet-}$ -induced degradation. Therefore, photodegradation
28 kinetics of Bz^- and AcPh should be slower in seawater (containing $[\text{Br}^-] \sim 1 \text{ mM}$) compared to
29 freshwaters. The present findings suggest that photochemistry would play a role both in the
30 formation of water-soluble organic compounds upon weathering of plastic particles, and in their
31 degradation.

32

33 **Keywords:** Environmental photochemistry; Photochemical fate; Kinetic constant; Polystyrene;
34 Aromatic compounds; Natural waters.

35

36 **1. Introduction**

37

38 Pollution by plastics is a growing environmental concern, especially for natural waters where plastic
39 inputs have reached alarming proportions. It has been calculated that approximately 6300 Mt of
40 plastic waste had been produced until 2015 and around 79% ($\sim 4977 \text{ Mt}$) was accumulated in
41 landfills or the natural environment (Geyer et al., 2017). The majority of plastic debris reaches the
42 sea through rivers, and different estimates have been performed to quantify the amount of plastic
43 transported by rivers to the sea. Such estimates range from 0.47 up to 12.7 million metric tons of
44 plastic per year (Jambeck et al., 2015; Schmidt et al., 2017).

45 Once they reach the natural environment, plastics undergo weathering largely due to the action of
46 sunlight that operates through two main processes. The former is sunlight-induced fragmentation of
47 plastic objects (macroplastics) into smaller particles, *i.e.*, micro- and finally nanoplastics (Andrady
48 et al., 2022). Adding to the primary environmental sources of small plastic particles (which include
49 their use in fertilizers and release upon runoff from artificial turf pitches; Kumar et al., 2020;
50 Salthammer, 2022), fragmentation highly affects environmental behaviour because of the reactivity

51 of small-sized plastics (Bianco et al., 2020). These can impact living organisms to a different degree
52 than macroplastics, for instance by reaching tissues and crossing membranes (Liu et al., 2021). The
53 second weathering process by sunlight is photodissolution, which consists in photoinduced release
54 to the water phase of additives or polymer fragmentation products (Gewert et al., 2015; Zhu et al.,
55 2020). The chemical compounds arising from plastic weathering can have adverse effects on living
56 organisms, in particular if they have endocrine-disruption properties (Burgos-Aceves et al., 2021).
57 These compounds might also play potential role as markers of plastic pollution, especially in cases
58 where plastics are difficult to detect, *e.g.*, because of their small size: nanoplastics are particularly
59 challenging as far as detection and polymer identification are concerned (Jakubowicz et al., 2021).
60 The environmental role of plastic weathering products is deeply affected by environmental
61 persistence. For instance, a persistent compound can undergo accumulation up to relatively high
62 concentration values, which enhances its effects and also makes quantification much easier.
63 However, it can also migrate quite far from the pollution source. Sunlight, in addition to being a
64 major driver of plastic weathering, would also play a role in the transformation of plastic
65 degradation products in natural surface waters. In particular, solar radiation would operate through
66 direct photolysis and indirect photochemistry (Guo et al., 2022). Direct photolysis occurs when a
67 compound absorbs sunlight, and the absorption process triggers transformation by, for instance,
68 ionisation, bond breaking, and excited-state reactivity (Katagi, 2018). In the case of indirect
69 photochemistry, sunlight is absorbed by naturally occurring photosensitisers such as nitrate, nitrite,
70 and chromophoric dissolved organic matter (CDOM). These species absorb sunlight and yield the
71 so-called photochemically produced reactive intermediates (PPRIs), of which the main ones are the
72 hydroxyl ($\bullet\text{OH}$) and carbonate ($\text{CO}_3^{\bullet-}$) radicals, singlet oxygen ($^1\text{O}_2$), and CDOM triplet states
73 ($^3\text{CDOM}^*$) (Yan and Song, 2014; Vione and Scozzaro, 2019). The photolysis of nitrate and nitrite
74 yields $\bullet\text{OH}$, while CDOM irradiation yields $^3\text{CDOM}^*$, $^1\text{O}_2$, as well as $\bullet\text{OH}$. $\text{CO}_3^{\bullet-}$ is produced by
75 oxidation of $\text{HCO}_3^-/\text{CO}_3^{2-}$ by $\bullet\text{OH}$, or CO_3^{2-} oxidation by $^3\text{CDOM}^*$ (Rosario-Ortiz and Canonica,

76 2016; McNeill and Canonica, 2016; Yan et al., 2019). The PPRI have very low steady-state
77 concentrations in sunlit natural waters (10^{-18} – 10^{-14} M), because they are quickly
78 scavenged/quenched by several processes. In particular: $\bullet\text{OH}$ is mainly scavenged by dissolved
79 organic matter (DOM, either chromophoric or not) and, usually to a lesser extent, by $\text{HCO}_3^-/\text{CO}_3^{2-}$;
80 $\text{CO}_3^{\bullet-}$ is mostly scavenged by DOM; $^3\text{CDOM}^*$ is mainly quenched by O_2 to produce $^1\text{O}_2$, with
81 ~50% yield; finally, $^1\text{O}_2$ is mostly quenched by collision with water (Gligorovski et al., 2015; Yan
82 et al., 2019; Ossola et al., 2021). In the case of saltwater and especially seawater, the main
83 scavenging process for $\bullet\text{OH}$ is the reaction with Br^- to eventually yield $\text{Br}_2^{\bullet-}$, which is also a PPRI
84 (Parker and Mitch, 2016). The budget between photoproduction and scavenging/quenching controls
85 PPRI occurrence in natural waters under sunlight. In particular, $\bullet\text{OH}$ and $\text{CO}_3^{\bullet-}$ tend to be more
86 concentrated at low values of the dissolved organic carbon (DOC), while the opposite happens in
87 the case of $^3\text{CDOM}^*$ and $^1\text{O}_2$ (Vione and Scozzaro, 2019). The higher is the steady-state
88 concentration of a PPRI, the higher is its ability to trigger transformation of dissolved compounds,
89 including those released by plastic weathering.

90 Previous studies have shown that weathering of polystyrene particles under sunlight yields a
91 number of dissolved compounds, among which benzoate (Bz^-) and acetophenone (AcPh) have been
92 identified as important photoproducts (Bianco et al., 2020). For these compounds, reactivity with
93 $\bullet\text{OH}$ and $\text{CO}_3^{\bullet-}$ can be assessed on the basis of the literature (Buxton et al., 1988; Neta et al., 1988;
94 Wols and Hofman-Caris, 2021), but no data are currently available for the other photoinduced
95 reactions. Therefore, the goal of this work is to assess the potential for abiotic degradation of both
96 compounds by direct and indirect photochemistry, with the purpose of better defining their fate in
97 the environment. In the case of semivolatile AcPh, we also consider its potential partitioning
98 between the liquid and the gas phase and, finally, its possible photodegradation in both surface
99 waters and the atmosphere. The reactivity of Bz^- and AcPh with $\text{Br}_2^{\bullet-}$ was also investigated, to
100 tentatively assess photodegradation of the two compounds in seawater vs. freshwater.

101 **2. Materials and Methods**

102

103 **2.1. Chemicals**

104 All reagents, solvents, and eluents were of analytical grade, or gradient-grade for liquid
105 chromatography. They were purchased from: Sigma-Aldrich (4-carboxybenzophenone, sodium
106 benzoate, acetophenone, 2-nitrobenzaldehyde, furfuryl alcohol, H₂O₂, NaNO₃, and NaBr); Alfa
107 Aesar (Rose Bengal and NaOH), and VWR International (acetonitrile, methanol, and H₃PO₄). The
108 mentioned chemicals were used as received, without further purification. Water was produced by a
109 Milli-Q apparatus (Millipore, resistivity 18.2 MΩ cm, TOC = 0.2 ppm).

110

111 **2.2. Irradiation experiments**

112 Solutions to be irradiated (5 mL total volume) were placed in cylindrical Pyrex glass cells (height
113 2.5 cm, diameter 4.0 cm, cut-off wavelength 280 nm), equipped with a lateral neck for liquid
114 insertion and withdrawal. The neck was tightly closed with a screw cap during the irradiation
115 experiments, in which solutions underwent magnetic stirring. Irradiation sources in different
116 experiments were a UVB lamp (Philips Narrowband TL20W/01 RS, emission maximum at 313
117 nm), a UVA lamp (black lamp TL-D 16W BLB, emission maximum at 369 nm), or a yellow lamp
118 (TL-D 18W/16, emission maximum at 580 nm). The UVB lamp was used to study the direct
119 photolysis of Bz⁻ and AcPh. The UVA lamp was used to achieve selective excitation of 4-
120 carboxybenzophenone (CBBP), which was employed as CDOM proxy to study the reactions with
121 ³CDOM*. Because previous studies have shown that ³CBBP* has comparable reactivity as average
122 ³CDOM* (Carena et al., 2019), CBBP irradiation can be used to assess the second-order reaction
123 rate constants between dissolved compounds and ³CDOM*, by means of steady-state irradiation
124 experiments. Finally, the yellow lamp was used for selective excitation of Rose Bengal, to produce
125 ¹O₂.

126 The spectral photon flux density in the solutions subject to irradiation was determined by a
127 combination of lamp spectral measurements (Ocean Optics USB2000 CCD spectrophotometer) and
128 chemical actinometry with 2-nitrobenzaldehyde (Bacilieri et al., 2022). Details are described in
129 **Text S1** of the Supplementary Material (hereinafter **SM**), which also reports the lamp spectra
130 (**Figure S1**).

131

132 **2.3. Instrumental analysis**

133 Absorption spectra were measured with a Varian Cary 100 Scan UV-Vis double-beam
134 spectrophotometer, using Hellma quartz cuvettes (1 cm optical path length).

135 After scheduled irradiation times, the cells were withdrawn from the lamp and their contents was
136 analysed by liquid chromatography (HPLC-UV). The instrument used was a Merck-Hitachi
137 chromatograph, equipped with AS2000A autosampler (60 μ L injection volume), L-6200 and L-
138 6000 pumps for high-pressure binary gradients, and L-4200 UV-Vis detector. The instrument
139 mounted a Merck LiChroCART® 125-4 column, packed with LiChrospher® 100 RP-18 (5 μ m).
140 Elution (1 mL min^{-1} flow rate) was carried out with a mixture of 40% acetonitrile and 60% water,
141 acidified with H_3PO_4 to pH 3. The combinations of detection wavelengths and retention times were
142 225 nm and 2.75 min for Bz^- , and 245 nm and 4.60 min for AcPh. 2-Nitrobenzaldehyde, used for
143 actinometry measurements, was determined with the same column eluting (1 mL min^{-1}) with a
144 mixture of 35% methanol and 65% acidified water (pH 3, H_3PO_4), with 7.3 min retention time and
145 detection at 258 nm.

146

147 **2.4. Laser flash photolysis experiments**

148 The fourth harmonic (266 nm) of a Quanta Ray GCR 130-01 Nd:YAG laser system was used to
149 generate and follow the reactivity of $\text{Br}_2^{\bullet-}$ in aqueous solution, in the presence of Bz^- and AcPh.
150 The excitation energy was 36 mJ/pulse and an individual cuvette sample (3 mL volume) was used

151 for a maximum of four consecutive laser shots. The spectroscopic system has been described before
152 (Brigante et al., 2014).

153 $\text{Br}_2^{\bullet-}$ was generated through photolysis of 10 mM H_2O_2 in the presence of 10 mM Br^- . Under such
154 conditions, the presence of a long-lived transient species absorbing from 270 to 550 nm with a
155 maximum at 360 nm ($\epsilon \sim 9.9 \times 10^3 \text{ M}^{-1} \text{ cm}^{-1}$) was assigned to the formation of $\text{Br}_2^{\bullet-}$ (Hug, 1981).

156 The second-order reaction rate constants of $\text{Br}_2^{\bullet-}$ with Bz^- and AcPh were determined from the
157 slopes of the regression lines of the logarithmic decays of the $\text{Br}_2^{\bullet-}$ transient (monitored at 360 nm),
158 as a function of the concentration of each selected aromatic compound (Stern-Volmer method). The
159 error was estimated as $\pm\sigma$, obtained from the scattering of the experimental data around the linear fit
160 line.

161

162 **2.5. Environmental fate modelling**

163 Photodegradation kinetics of Bz^- and AcPh were modelled with the APEX software (Aqueous
164 Photochemistry of Environmentally-occurring Xenobiotics) (Vione, 2020). This software predicts
165 pseudo-first order photodegradation rate constants by direct photolysis and indirect photochemistry,
166 as a function of sunlight irradiance, water depth, and water chemistry (concentration values of
167 photochemically relevant compounds: nitrate, nitrite, bicarbonate, carbonate, and dissolved organic
168 carbon, DOC) (Silva et al., 2015; Silva et al, 2019; Vione, 2020). APEX assumes well-mixed water
169 bodies under clear-sky conditions, and in these circumstances it has been shown to predict
170 environmental photodegradation kinetics with good accuracy (Avetta et al., 2016).

171 The volatilisation rate constant of AcPh from aqueous environments was predicted with the
172 EPISUITETM package by US-EPA (US-EPA, 2021), based on molecular structure (quantitative
173 structure-activity relationship). Water depth was varied in the range of 1 to 5 m, while it was
174 assumed 1 m s^{-1} wind speed. EPISUITETM (AOPWIN sub-package) was also used for the

175 prediction of the reaction rate constant between AcPh and gas-phase $\bullet\text{OH}$, assuming average
176 $[\bullet\text{OH}_{(\text{g})}] = 1.5 \times 10^6 \text{ cm}^{-3}$.

177

178 3. Results and Discussion

179

180 To assess the photochemical degradation potential of Bz^- and AcPh, all the reaction rate constants
181 with photochemically produced reactive intermediates (PPRIs) and the direct photolysis quantum
182 yields need to be retrieved from literature, or measured through laboratory experiments.

183 The second-order reaction rate constants of Bz^- and AcPh with $\bullet\text{OH}$ are known from the literature,
184 and they are both equal to $5.9 \times 10^9 \text{ M}^{-1} \text{ s}^{-1}$ (Buxton et al., 1988; Wolf and Hofman-Caris, 2012).
185 Furthermore, Bz^- is known not to react with $\text{CO}_3^{\bullet-}$ to a significant extent (Vione et al., 2010;
186 Wojnárovits et al., 2020), while AcPh has a kinetic constant with $\text{CO}_3^{\bullet-}$ of $k_{\text{AcPh},\text{CO}_3^{\bullet-}} = 1 \times 10^7 \text{ M}^{-1}$
187 s^{-1} (Neta et al., 1988).

188 Irradiation experiments, carried out in the framework of this work, allowed for excluding significant
189 reactions of the studied compounds with either $^3\text{CBBP}^*$ (and, therefore, $^3\text{CDOM}^*$) or $^1\text{O}_2$.

190 Differently from Bz^- , AcPh was found to undergo direct photolysis to a significant extent under the
191 UVB lamp. UVB irradiation of $5 \mu\text{M}$ AcPh (pH 7, phosphate buffer) produced degradation with
192 pseudo-first order kinetics, and initial degradation rate $R_{\text{AcPh}} = (4.94 \pm 1.02) \times 10^{-12} \text{ M s}^{-1}$, while no
193 AcPh degradation was observed in the dark. The UVB photon flux absorbed by AcPh (Braslavsky,
194 2007) was determined as $P_{\text{a,AcPh}} = \int_{\lambda} p^{\circ}(\lambda) [1 - 10^{-\varepsilon_{\text{AcPh}}(\lambda) \times b \times C_{\text{AcPh}}}] d\lambda = 5.3 \times 10^{-8} \text{ Einstein L}^{-1} \text{ s}^{-1}$,

195 where $p^{\circ}(\lambda)$ is the spectral photon flux density (measured by chemical actinometry) that passes
196 through the irradiated solutions (**Figure S1, SM**), $\varepsilon_{\text{AcPh}}(\lambda)$ the molar absorption coefficient of AcPh
197 (**Figure S1, SM**), $b = 0.4 \text{ cm}$ the optical path length of the irradiated solutions, and $C_{\text{AcPh}} = 5 \mu\text{M}$.

198 The direct photolysis quantum yield of AcPh was calculated as $\Phi_{\text{AcPh}} = R_{\text{AcPh}} (P_{\text{a,AcPh}})^{-1} =$
199 $(9.2 \pm 1.9) \times 10^{-5} \text{ mol Einstein}^{-1}$.

200

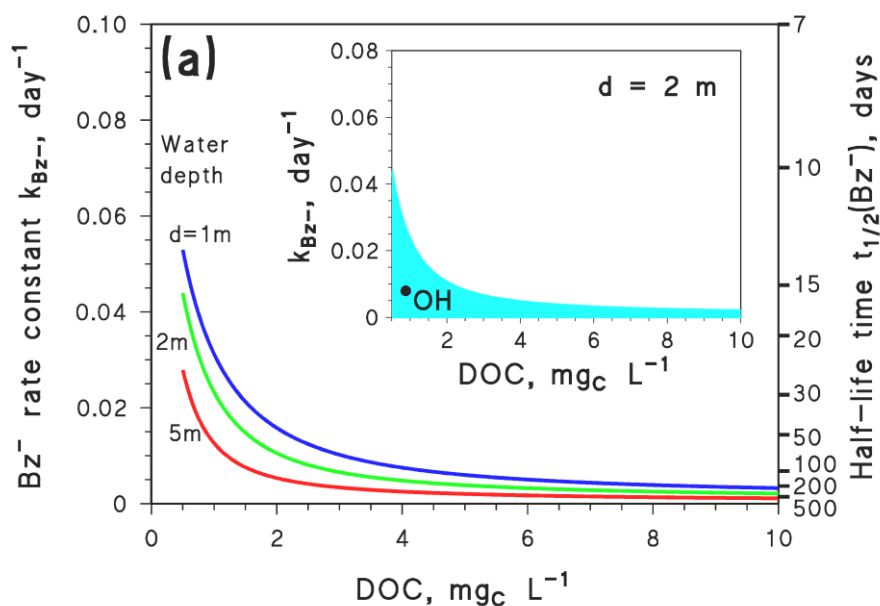
201 **3.1. Photochemical persistence of Bz⁻ and AcPh in natural surface waters**

202

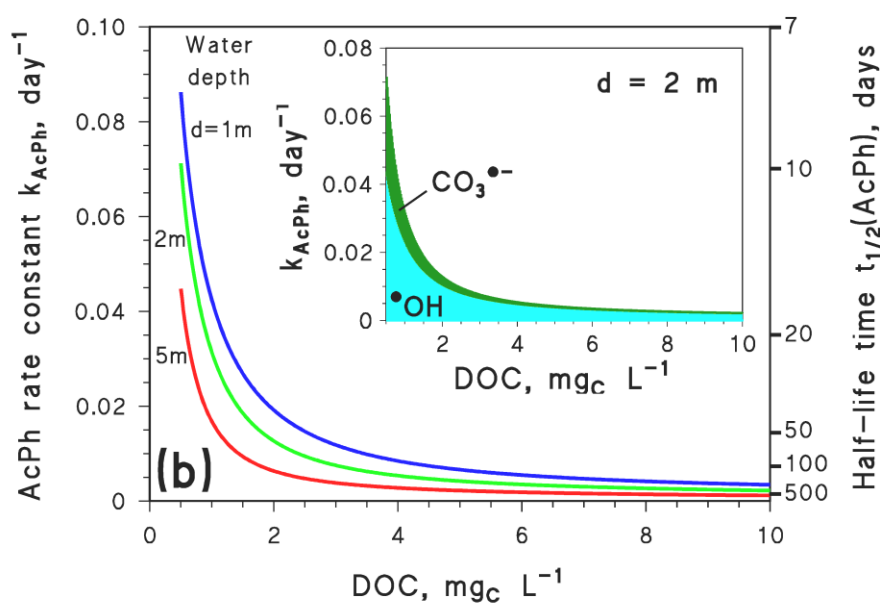
203 Based on the above photoreaction parameters, the photochemical degradation kinetics of Bz⁻ and
204 AcPh in sunlit natural waters was assessed by means of the APEX software (see **Figure 1**). The
205 assumed conditions of sunlight irradiation ('day') correspond to the 24-h-round spring equinox at
206 45°N latitude. As such, they also represent reasonable year averages at mid latitude under fair-
207 weather conditions (Vione, 2020). Calculation results suggest that AcPh direct photolysis would
208 play minor role, thus Bz⁻ would be photodegraded by •OH and AcPh would react with both •OH
209 and CO₃^{•-}. Predicted photodegradation lifetimes range from 1-2 weeks to several months.

210 Photodegradation kinetics would be highly dependent on the environmental conditions. Kinetics
211 would be the fastest in shallow waters with low DOC, because: (i) shallow waters are better
212 illuminated by sunlight than deep waters (Loiselle et al., 2008), the bottom layer of which is usually
213 in the dark, and (ii) organic matter is a major scavenger of both •OH and CO₃^{•-} (Yan et al., 2019)
214 and it acts as a light-screening agent that prevents the direct photolysis of other compounds,
215 including the photosensitisers nitrate and nitrite. Therefore, kinetics of photodegradation by •OH
216 and CO₃^{•-} are slower at high DOC values.

217 The important role played by •OH and/or CO₃^{•-} in the photodegradation of Bz⁻ and AcPh suggests
218 that nitrate concentration might affect phototransformation kinetics considerably. Nitrate is in fact a
219 direct •OH and indirect CO₃^{•-} source (Vione and Scozzaro, 2019) and, as shown in **Figure S2**
220 **(SM)**, the pseudo-first order rate constants of both Bz⁻ and AcPh increase with increasing nitrate,
221 all other conditions being equal.



222



223

224 **Figure 1.** Modelled first-order phototransformation rate constants (k , left Y-axis), and corresponding half-
 225 life times ($t_{1/2} = \ln 2 k^{-1}$; right Y-axis) as a function of the DOC, for different values of the water depth d : **(a)**
 226 Bz^- ; **(b)** AcPh. Other water parameters: 10^{-4} M NO_3^- , 10^{-6} M NO_2^- , 10^{-3} M HCO_3^- , and 10^{-5} M CO_3^{2-} . The
 227 relative importance of the different photoreaction pathways is shown as figure inserts (2 m depth). The
 228 phototransformation of Bz^- is predicted to take place by reaction with $\bullet OH$ only. Assumed sunlight
 229 irradiation corresponds to the spring equinox at $45^\circ N$ latitude, under fair-weather conditions.

230

231 The nitrate effect is substantial at low DOC (increase by 4-5 times in degradation kinetics when
232 passing from 10^{-6} M to 10^{-4} M NO_3^- , for $\text{DOC} = 1 \text{ mg}_C \text{ L}^{-1}$; **Figure S2**), while the effect is much
233 less important at higher DOC values. The rationale is that high DOC entails the scavenging by
234 DOM of the vast majority of $\bullet\text{OH}$ and $\text{CO}_3^{\bullet-}$ photogenerated by nitrate.

235

236 **3.2. Possible environmental scenarios**

237 Different scenarios of photoinduced degradation in the environment were taken into account for the
238 studied compounds. In the case of non-volatile Bz^- we have considered photodegradation in surface
239 waters only. Bz^- formation kinetics from polystyrene exposed to sunlight has been studied
240 previously (Bianco et al., 2020) and the available data allow for describing a possible scenario
241 where polystyrene degradation yields Bz^- , which is then photodegraded by $\bullet\text{OH}$. By so doing, it is
242 possible to assess a potential for Bz^- accumulation in natural waters. In the case of semivolatile
243 AcPh, we simulated a scenario of degradation in both surface waters and the atmosphere, combined
244 with AcPh volatilisation from the aqueous phase to the gas phase.

245

246 **3.2.1. Benzoate (Bz^-)**

247 In the case of Bz^- , formation kinetics from 0.2% v/v polystyrene in water under environmental
248 irradiation is known (Bianco et al., 2020), which would be representative of strong water pollution
249 by polystyrene particles. The scenario considered here assumes that polystyrene particles occur near
250 the water surface (*i.e.*, they float), while released Bz^- undergoes diffusion in the whole water
251 volume. In addition, it is assumed that Bz^- is degraded by reaction with $\bullet\text{OH}$ (see **Figure 1a**),
252 following first-order kinetics. Details of kinetic calculations are provided in **Text S2** of SM. The
253 time trend of Bz^- that results from the formation-photodegradation budget is the following:

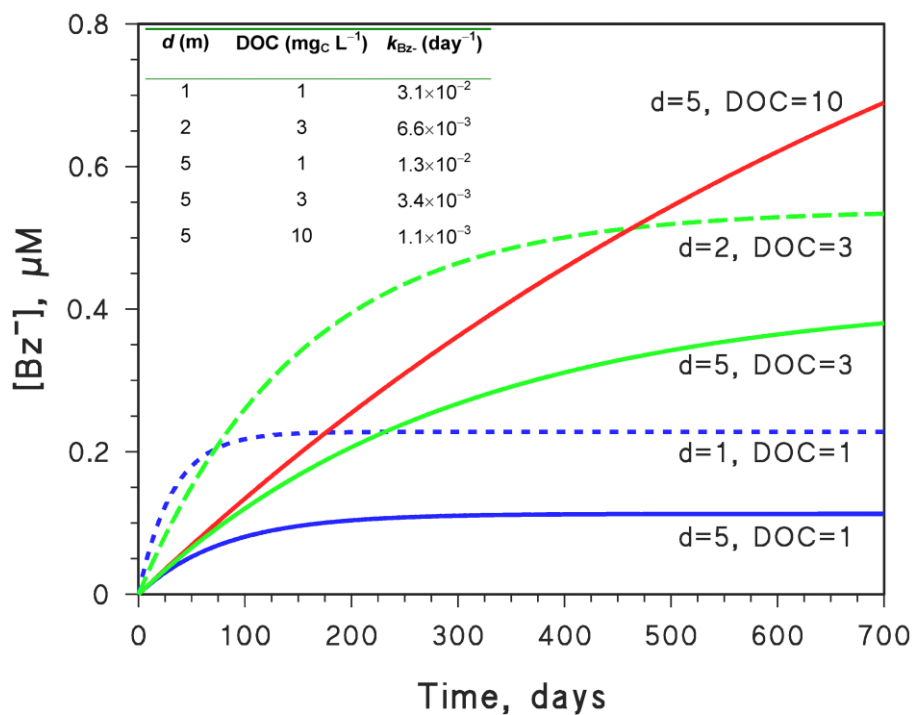
$$254 \quad [\text{Bz}^-] = \frac{R_{\text{Bz}^-} - d_o}{k_{\text{Bz}^-} - d} (1 - e^{-k_{\text{Bz}^-} t}) \quad (1)$$

255 where $R_{\text{Bz}^-} = 3.1 \times 10^{-7} \text{ M day}^{-1}$ and $d_o = 0.023 \text{ m}$ are derived from the literature (Bianco et al.,
256 2020). They are, respectively, the experimental formation rate of Bz^- from polystyrene and the
257 experimental water depth, see also **Text S2**. Furthermore, d [m] is the assumed depth of the water
258 body, k_{Bz^-} [day^{-1}] the pseudo-first order degradation rate constant of Bz^- (modelled with APEX),
259 and t is time in days.

260 To simplify calculations, as an approximation we kept k_{Bz^-} constant with time at its equinox value
261 (yearly average). In other words, the value of k_{Bz^-} we used varied in different conditions of, *e.g.*,
262 water depth (d) and DOC as per **Figure 1a**, but its seasonal fluctuations were neglected. Seasonal
263 variations were neglected also in the case of R_{Bz^-} , which is a year average as well. Considering that
264 polystyrene releases Bz^- under irradiation and that Bz^- would react with photogenerated $\bullet\text{OH}$, it is
265 likely that R_{Bz^-} and k_{Bz^-} vary in parallel and that their seasonal variations cancel out at least partially
266 in **Eq. (1)**. With these approximations, the Bz^- time trends in different conditions are shown in
267 **Figure 2**.

268 **Eq. (1)** predicts that $[\text{Bz}^-]$ reaches a plateau after quite long time (high t values). The plateau
269 concentration results from the budget between generation from polystyrene and degradation by
270 $\bullet\text{OH}$. Furthermore, the initial increase in $[\text{Bz}^-]$ (low t values, $t < 50$ days) mostly depends on water
271 depth d : if water is deep, generated Bz^- is diluted in a higher volume, and its concentration increase
272 is slower (and *vice versa*, in the case of shallow water). At later times, water depth has two opposite
273 impacts on the Bz^- time trend, which partially offset each other (**Text S2**): the former is the dilution
274 effect, already mentioned; the latter is the fact that the deeper is water, the slower is Bz^- degradation
275 upon reaction with $\bullet\text{OH}$ (see **Figure 1a**).

276 The plateau concentration of Bz^- strongly depends on the DOC: if DOC is high, Bz^- degradation is
277 slow and $[\text{Bz}^-]$ can reach higher values with potential accumulation; the opposite happens at low
278 DOC.



279

280 **Figure 2.** Time trends of Bz^- in different surface-water scenarios, as predicted by **Eq. (1)**. The value of k_{Bz^-}
 281 in each condition (see the table insert) was referred to the spring equinox under clear sky. The measure unit
 282 of the DOC value reported near each curve is [$\text{mg}_C \text{ L}^{-1}$], that of d (water depth) is [m]. Other water
 283 conditions for the APEX modelling of k_{Bz^-} are as follows: 10^{-4} M NO_3^- , 10^{-6} M NO_2^- , $10^{-3} \text{ M HCO}_3^-$, and
 284 $10^{-5} \text{ M CO}_3^{2-}$.

285

286

287 As shown in **Figure 2**, Bz^- would eventually reach sub- μM levels. By comparison, in the literature
 288 experiment that yielded $R_{Bz^-} = 3.1 \times 10^{-7} \text{ M day}^{-1}$ (Bianco et al., 2020) the volume was quite small (d
 289 = 0.023 m, thereby ensuring limited dilution) and the aqueous phase did not contain $\bullet\text{OH}$ sources. In
 290 such circumstances, Bz^- could accumulate with little dilution or degradation and reach 0.13 mM
 291 levels in 14 months. In the current simulations, for water depths of some metres and in the presence
 292 of Bz^- degradation by $\bullet\text{OH}$, we predict $[Bz^-]$ to reach values that are lower by 2-3 orders of
 293 magnitude (sub- μM vs. sub-mM), which looks reasonable.

294

295 3.2.2. Acetophenone (AcPh)

296 As mentioned before, AcPh could be degraded in water by (mainly) $\bullet\text{OH}$ and $\text{CO}_3^{\bullet-}$, or volatilise to
297 the gas phase where it would react with $\bullet\text{OH}_{(g)}$, similarly to other semivolatile compounds (Arsene
298 et al., 2022). The overall scenario is depicted in **Scheme 1a**, and two specific scenarios are
299 illustrated in **Scheme 1b**.

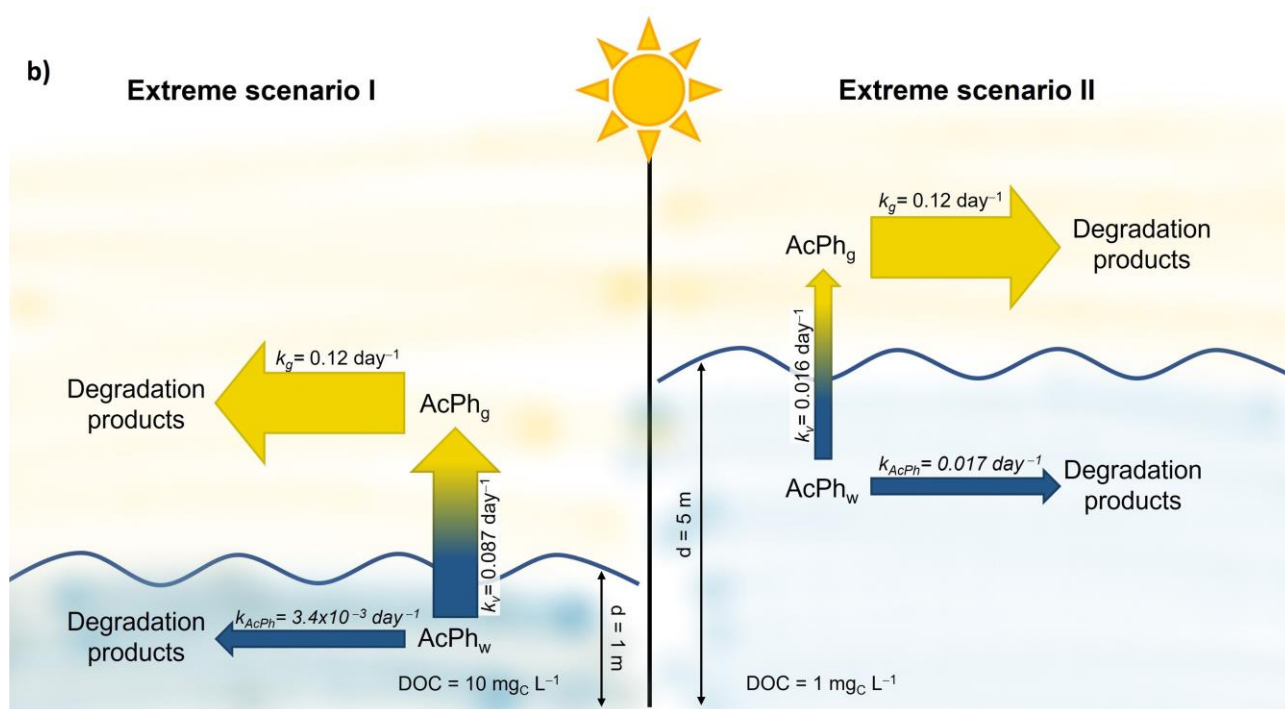
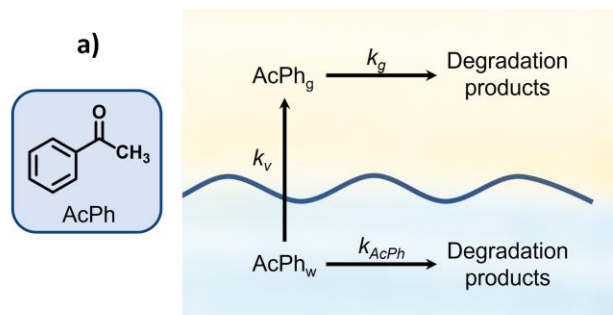
300 Starting from AcPh in water (AcPh_w) at initial concentration C_o , the kinetic system depicted in
301 **Scheme 1** gives the following time trends for $[\text{AcPh}_w]$ and $[\text{AcPh}_g]$ (w = water phase, g = gas
302 phase). **Equations (2,3)** are solutions of differential equations and were derived in similar way as
303 Arsene et al. (2022) (see **Scheme 1** for the meaning of the different parameters):

$$304 \quad [\text{AcPh}_w] = C_o e^{-(k_{\text{AcPh}}+k_v)t} \quad (2)$$

$$305 \quad [\text{AcPh}_g] = \frac{k_v C_o}{k_g - k_{\text{AcPh}} - k_v} [e^{-(k_{\text{AcPh}}+k_v)t} - e^{-k_g t}] \quad (3)$$

306 The values of k_{AcPh} as a function of water depth and DOC were modelled with APEX (see **Figure**
307 **1b**); k_g was assessed as 0.12 day^{-1} by EpiSuite 4.1 (AOPWIN), assuming average $[\bullet\text{OH}_{(g)}] = 1.5 \times 10^6$
308 cm^{-3} ; finally, the estimated value of k_v (0.016 - 0.087 day^{-1} ; EpiSuite 4.1) depends on water depth and
309 is lower as d is higher ($1 < d < 5 \text{ m}$, see **Figure S4** in SM).

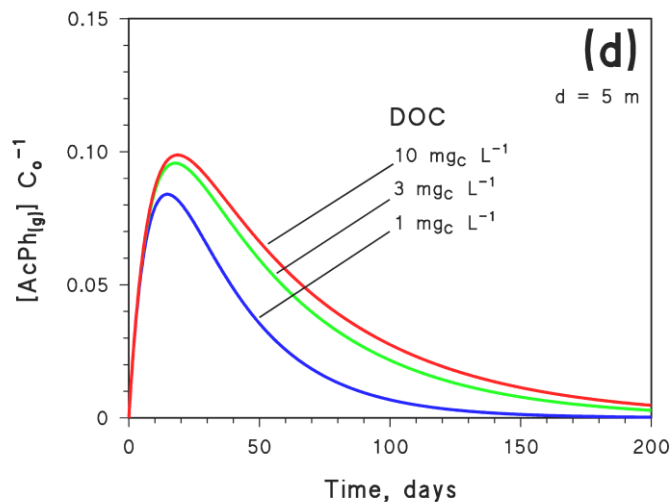
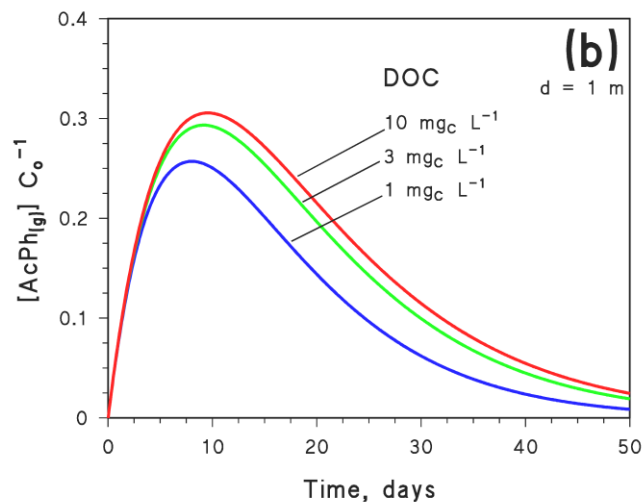
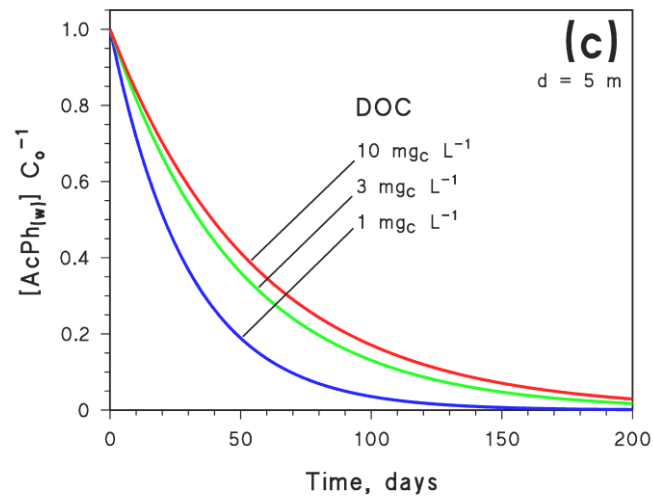
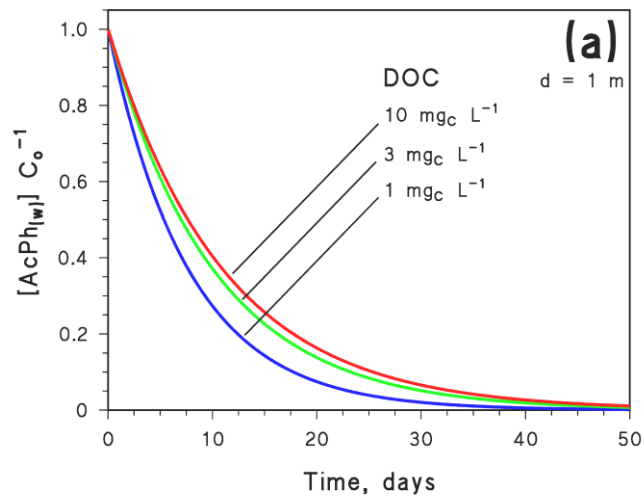
310 The time trends of $[\text{AcPh}_w]$ and $[\text{AcPh}_g]$, obtained according to **Eqs. (2)** and **(3)**, are shown in
311 **Figure 3** for different values of the water depth d (1 or 5 m) and of the DOC (1, 3, or $10 \text{ mg}_C \text{ L}^{-1}$).
312 A first issue is that volatilisation would usually play the main role in the removal of AcPh from the
313 aqueous phase, except for $d = 5 \text{ m}$ and $\text{DOC} = 1 \text{ mg}_C \text{ L}^{-1}$ where volatilisation and photodegradation
314 would be comparable (**Scheme 1b**). Because of the important weight of k_v in **Eq. (2)**, the DOC
315 value (which only affects k_{AcPh}) would have relatively limited effect on the time trend of $[\text{AcPh}_w]$
316 (**Figure 3a,c**). Furthermore, removal kinetics of AcPh from the aqueous phase would be
317 considerably faster at $d = 1 \text{ m}$ (where k_{AcPh} and especially k_v are considerably higher, see **Figure 3a**
318 and **Scheme 1b**) than at $d = 5 \text{ m}$ (**Figure 3c**).



319

320

321 **Scheme 1.** In **a)** overall reaction scheme of AcPh in the aqueous phase (w) and in the gas phase (g). The
 322 pseudo-first order AcPh rate constants are also shown: k_{AcPh} is the photodegradation rate constant in water,
 323 modelled with APEX; k_v is the volatilisation rate constant, modelled with EpiSuite 4.1; k_g is the degradation
 324 rate constant upon reaction with $\bullet OH_{(g)}$, also modelled with EpiSuite 4.1 (AOPWIN). In **b)** are represented
 325 two extreme scenarios: scenario I is characterised by water depth $d = 1$ m and $DOC = 10 \text{ mg}_C \text{ L}^{-1}$, scenario
 326 II assumes $d = 5$ m and $DOC = 1 \text{ mg}_C \text{ L}^{-1}$. The arrow sizes are roughly proportional to the rate constant
 327 values.



328

329

330

331

Figure 3. Modelled time trends of $[\text{AcPh}_w]$ ((a,c), Eq. (2)) and $[\text{AcPh}_g]$ ((b,d), Eq. (3)), for different values of the DOC and for water depth $d = 1$ m (a,b) and 5 m (c,d). Other water conditions: 10^{-4} M NO_3^- , 10^{-6} M NO_2^- , 10^{-3} M HCO_3^- , and 10^{-5} M CO_3^{2-}

332 The initial increase of $[\text{AcPh}_g]$ is controlled by k_v and, therefore, it does not depend on the DOC
333 (**Figure 3b,d**). The gas-phase degradation of AcPh is also DOC-independent, because $k_g = 0.12$
334 day^{-1} is only linked to the value of $[\bullet\text{OH}_{(g)}]$. In spite of these issues, there are some differences in
335 the $[\text{AcPh}_g]$ time trends (**Figure 3b,d**), which depend on the DOC value of the aqueous phase. The
336 reason is that low DOC entails slightly faster decay of AcPh_w (**Figure 3a,c**), because of higher
337 values of $[\bullet\text{OH}]$ and $[\text{CO}_3^{\bullet-}]$ in the aqueous phase that lead to higher k_{AcPh} . As AcPh_w undergoes
338 slightly faster consumption at low DOC, a lesser amount is available for partitioning to the gas
339 phase and, therefore, AcPh_g reaches slightly lower concentration values if the water DOC is low
340 (**Figure 3b,d**).

341 Overall, model results suggest that volatilisation and reaction with gas-phase $\bullet\text{OH}$ have potential to
342 play key roles in the environmental fate of AcPh.

343

344 **3.3. Reactivity with $\text{Br}_2^{\bullet-}$, and implications for photodegradation in seawater**

345

346 The radicals $\bullet\text{OH}$ and $\text{CO}_3^{\bullet-}$ are expected to play important roles in the photodegradation of Bz^-
347 (only $\bullet\text{OH}$) and AcPh (both species) in sunlit freshwaters. However, in the case of brackish waters
348 and saltwater, $\bullet\text{OH}$ would be very effectively scavenged by bromide (Buxton et al., 1988; Parker
349 and Mitch, 2016). This phenomenon would strongly inhibit the $\bullet\text{OH}$ -mediated processes, and it
350 would also block the main $\text{CO}_3^{\bullet-}$ formation pathway ($\text{HCO}_3^-/\text{CO}_3^{2-}$ oxidation by $\bullet\text{OH}$ itself;
351 Canonica et al., 2005). At the same time, the reactive radical $\text{Br}_2^{\bullet-}$ would be generated by $\bullet\text{OH}$ in
352 the presence of bromide (Parker and Mitch, 2016): the main processes connected with the
353 occurrence of $\text{Br}_2^{\bullet-}$ in environmental waters are depicted in **Scheme 2**.

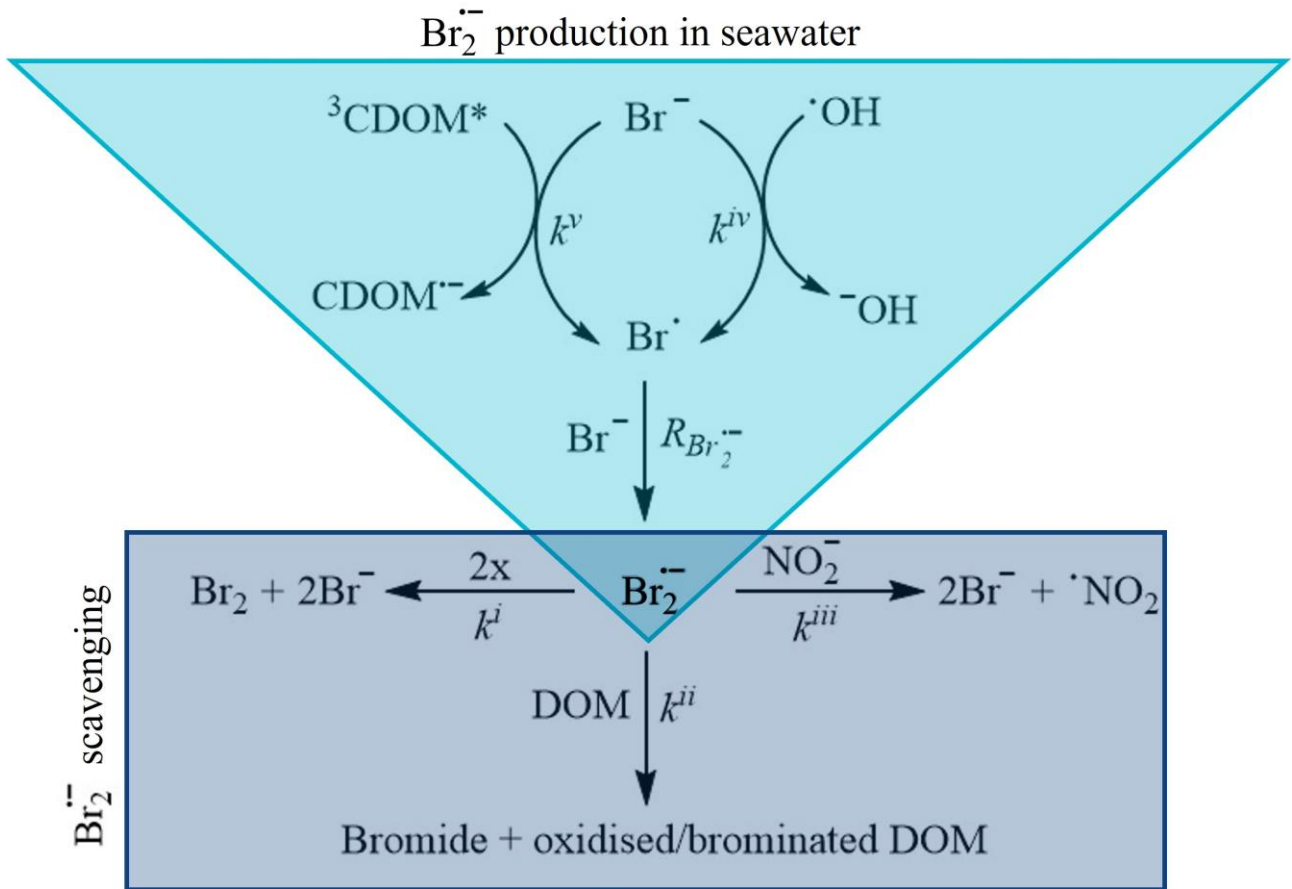
354 Based on **Scheme 2**, and applying the steady-state approximation to both Br^\bullet and $\text{Br}_2^{\bullet-}$, one gets the
355 following equations for, respectively, $\text{Br}_2^{\bullet-}$ formation rate and its steady-state concentration (De
356 Laurentiis et al., 2012):

357 $R_{Br_2^{\bullet-}} = [Br^-] (k^{iv} [\bullet OH] + k^v [{}^3CDOM^*])$ (4)

358 $[Br_2^{\bullet-}] = \frac{-(k^{ii} DOC + k^{iii} [NO_2^-]) + \sqrt{(k^{ii} DOC + k^{iii} [NO_2^-])^2 + 4k^i R_{Br_2^{\bullet-}}}}{2k^i}$ (5)

359 where the reaction rate constants k^i - k^v are those shown in **Scheme 2**.

360



361

362

363 **Scheme 2.** Main reactions accounting for the production (in the light blue triangle) and

364 scavenging/quenching (in the dark blue rectangle) of $Br_2^{\bullet-}$ in bromide-containing natural waters. The

365 relevant rate constants are those used in **Equations (4,5)**: $k^i = 2 \times 10^9 \text{ M}^{-1} \text{ s}^{-1}$, $k^{ii} = 306 \text{ L mg}_C^{-1} \text{ s}^{-1}$, $k^{iii} =$

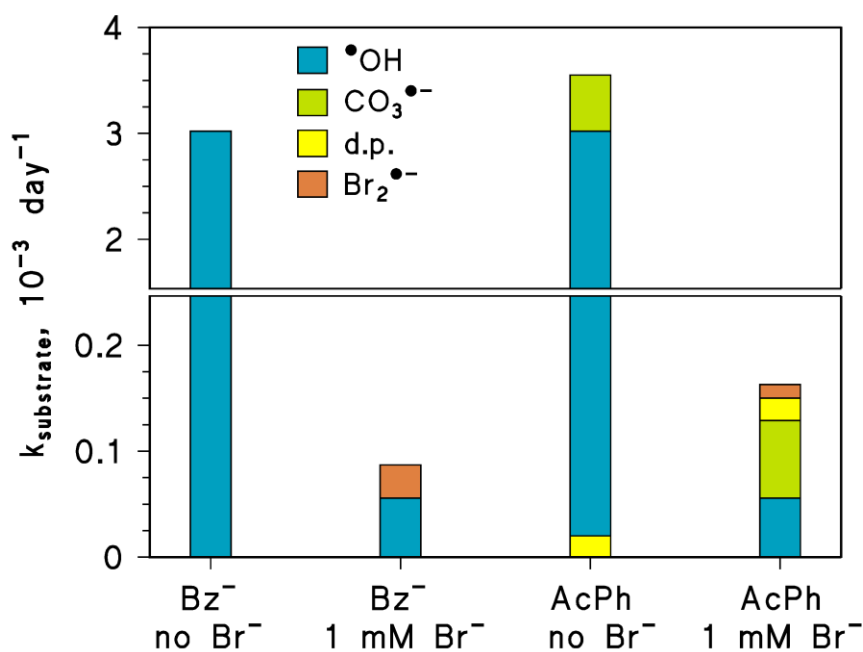
366 $2 \times 10^7 \text{ M}^{-1} \text{ s}^{-1}$, $k^{iv} = 1.1 \times 10^{10} \text{ M}^{-1} \text{ s}^{-1}$, and $k^v = 3 \times 10^9 \text{ M}^{-1} \text{ s}^{-1}$ (see De Laurentiis et al., 2012).

367

368 $\text{Br}_2^{\bullet-}$ is quite reactive and might have a role in degradation reactions. Therefore, it is very
369 interesting to assess the reactivity of the studied compounds with $\text{Br}_2^{\bullet-}$. Laser flash photolysis
370 experiments (see **Figure S5** in SM) yielded $k_{\text{Bz}^-, \text{Br}_2^{\bullet-}} = (4.8 \pm 0.5) \times 10^7 \text{ M}^{-1} \text{ s}^{-1}$ and $k_{\text{AcPh}, \text{Br}_2^{\bullet-}} =$
371 $(2.0 \pm 0.5) \times 10^7 \text{ M}^{-1} \text{ s}^{-1}$ as the second-order reaction rate constants of $\text{Br}_2^{\bullet-}$ with, respectively, Bz^-
372 and AcPh.

373 On the basis of the $\text{Br}_2^{\bullet-}$ second-order reaction rate constants obtained by laser flash photolysis, it is
374 possible to assess the first-order rate constants of degradation by $\text{Br}_2^{\bullet-}$ as $k_{\text{Substrate}} =$
375 $k_{\text{Substrate}, \text{Br}_2^{\bullet-}} \times [\text{Br}_2^{\bullet-}]$, where ‘Substrate’ = Bz^- or AcPh. The effect of bromide on the overall
376 kinetics (pseudo-first order rate constants) and on the different pathways of Bz^- and AcPh
377 degradation is shown in **Figure 4**.

378 First of all, 1 mM bromide (relevant to seawater conditions; Fukushi et al., 2000) would slow down
379 photodegradation of both compounds by over ten times. The $\bullet\text{OH}$ pathway would be particularly
380 affected, due to $\bullet\text{OH}$ scavenging by Br^- , followed by $\text{CO}_3^{\bullet-}$ that would also be inhibited
381 considerably. Although both Bz^- and AcPh would be degraded by $\text{Br}_2^{\bullet-}$ to a significant extent in the
382 presence of 1 mM Br^- , this process would be unable to offset inhibition of the $\bullet\text{OH}$ and $\text{CO}_3^{\bullet-}$
383 pathways. Therefore, Bz^- and AcPh are potentially more photostable in saline waters than in
384 freshwater.



385
386

387 **Figure 4.** Modelled pseudo-first order photodegradation rate constants of Bz⁻ and AcPh, in the absence of
388 bromide and in the presence of 1 mM bromide. The colour code highlights the different photoreaction
389 pathways: hydroxyl ($\bullet\text{OH}$) and carbonate ($\text{CO}_3^{\bullet-}$) radicals, dibromide radical anions ($\text{Br}_2^{\bullet-}$), and direct
390 photolysis (d.p.). APEX was used to calculate reaction kinetics by $\bullet\text{OH}$, $\text{CO}_3^{\bullet-}$, and the direct photolysis in
391 all conditions, and to assess $[\bullet\text{OH}]$ and $[\text{}^3\text{CDOM}^*]$ for the calculation of $R_{\text{Br}_2^{\bullet-}}$ and $[\text{Br}_2^{\bullet-}]$ (**Equations**
392 **(4,5)**). Other conditions (relevant to coastal seawater; Chen, 2001): 5 m depth, 3.5 mg_C L⁻¹ DOC, 10⁻⁵ M
393 NO₃⁻, 10⁻⁷ M NO₂⁻, 2.5×10⁻³ M HCO₃⁻, and 2.5×10⁻⁵ M CO₃²⁻. Assumed sunlight irradiation corresponds to
394 the spring equinox at 45°N latitude, under fair-weather conditions. Note the break in the Y-axis.

395

396 **4. Conclusions**

397

398 The experimental data obtained in this work allowed for excluding that direct photolysis or
399 reactions with $^1\text{O}_2$ or $^3\text{CDOM}^*$ could play significant role in the environmental fate of Bz^- and
400 AcPh in sunlit freshwaters. In contrast, photochemical modelling showed that $\bullet\text{OH}$ would contribute
401 to the environmental attenuation of Bz^- , while $\bullet\text{OH}$ and $\text{CO}_3^{\bullet-}$ would take part in the transformation
402 of AcPh . Such photoreaction pathways would be enhanced in the presence of low DOC or high
403 nitrate levels, while high DOC would protect the studied compounds from photodegradation. High
404 nitrate, which enhances photodegradation of both Bz^- and AcPh , is relevant to plastic pollution
405 because the spreading of fertilisers (of which nitrate is an important component) plays major role in
406 the occurrence of microplastics in surface waters (Kumar et al., 2020).

407 Differently from Bz^- , AcPh is volatile enough to undergo phase transfer from surface waters to the
408 atmosphere, where it could react with gas-phase $\bullet\text{OH}$. Such a process could be highly competitive
409 with the aqueous-phase photodegradation of AcPh by $\bullet\text{OH}$ and $\text{CO}_3^{\bullet-}$. Finally, although there is
410 potential for $\text{Br}_2^{\bullet-}$ to play significant role in the photodegradation of both Bz^- and AcPh at seawater
411 bromide levels, the scavenging of $\bullet\text{OH}$ by bromide would slow down considerably
412 photodegradation kinetics of both Bz^- and AcPh . Therefore, Bz^- and AcPh photodegradation should
413 be much slower in seawater compared to freshwaters.

414

415 **Acknowledgements**

416 This work is part of a project that has received funding from the European Research Council (ERC)
417 under the European Union's Horizon 2020 research and innovation program, grant agreement No
418 948666 – ERC-2020-StG NaPuE, from Fondazione CRT Erogazioni Ordinarie 2020 n. 2020.1874,
419 and from MIUR Call FARE project NATtA n. R20T85832Z.

420 **References**

421

422 Andrady, A. L., Barnes, P. W., Bornman, J. F., Gouin, T., Madronich, S., White, C. C., Zepp, R. G.,
423 Jansen, M. A. K., 2022. Oxidation and fragmentation of plastics in a changing environment;
424 from UV-radiation to biological degradation. *Sci. Total Environ.* 851(2), 158022.

425 Arsene, C., Bejan, I. G., Roman, C., Olariu, R. I., Minella, M., Passananti, M., Carena, L., Vione,
426 D., 2022. Evaluation of the environmental fate of a semivolatile transformation product of
427 ibuprofen based on a simple two-media fate model. *Environ Sci Technol.* 56, 15650-15660.

428 Avetta, P., Fabbri, D., Minella, M., Brigante, M., Maurino, V., Minero, C., Pazzi, M., Vione, D.,
429 2016. Assessing the phototransformation of diclofenac, clofibrac acid and naproxen in surface
430 waters: Model predictions and comparison with field data. *Water Res.* 105, 383-394.

431 Bacilieri, F., Vähätalo, A. V., Carena, L., Wang, M., Gao, P., Minella, M., Vione, D., 2022.
432 Wavelength trends of photoproduction of reactive transient species by chromophoric
433 dissolved organic matter (CDOM), under steady-state polychromatic irradiation.
434 *Chemosphere* 306, 135502.

435 Bianco, A., Sordello, F., Ehn, M., Vione, D., Passananti, M., 2020. Degradation of nanoplastics in
436 the environment: Reactivity and impact on atmospheric and surface waters. *Sci. Total*
437 *Environ.* 742, 140413.

438 Braslavsky, S.E., 2007. Glossary of terms used in photochemistry. third edition. *Pure and Applied*
439 *Chemistry* 79, 293-465.

440 Brigante, M., Minella, M., Mailhot, G., Maurino, V., Minero, C., Vione, D., 2014. Formation and
441 reactivity of the dichloride radical ($\text{Cl}_2^{\bullet-}$) in surface waters: a modelling approach.
442 *Chemosphere* 95, 464-469.

443 Burgos-Aceves, M. A., Abo-Al-Ela, H. G., Faggio, C., 2021. Physiological and metabolic approach
444 of plastic additive effects: Immune cells responses. *J. Hazard. Mater.* 404(A), 124114.

445 Buxton, G. V., Greenstock, C. L., Helman, P. W., Ross, A. B., 1988. Critical review of rate
446 constants for reactions of hydrated electrons, hydrogen atoms and hydroxyl radicals
447 ($\bullet\text{OH}/\bullet\text{O}^-$) in aqueous solution. *J. Phys. Chem. Ref. Data* 17, 513–886.

448 Canonica, S., Kohn, T., Mac, M., Real, F.J., Wirz, J., Von Gunten, U., 2005. Photosensitizer
449 method to determine rate constants for the reaction of carbonate radical with organic
450 compounds. *Environ. Sci. Technol.* 39, 9182–9188.

451 Carena, L., Puscasu, C. G., Comis, S., Sarakha, M., Vione, D., 2019. Environmental
452 photodegradation of emerging contaminants: A re-examination of the importance of triplet-

453 sensitised processes, based on the use of 4-carboxybenzophenone as proxy for the
454 chromophoric dissolved organic matter. *Chemosphere* 237, 124476.

455 Chen, C. T. A., 2001. General chemistry of seawater. *Oceanography Vol. I*, UNESCO-EOLSS, pp.
456 1-26.

457 De Laurentiis, E., Minella, M., Maurino, V., Minero, C., Mailhot, G., Sarakha, M., Brigante, M.,
458 Vione, D., 2012. Assessing the occurrence of the dibromide radical ($\text{Br}_2^{\bullet-}$) in natural waters:
459 measures of triplet-sensitised formation, reactivity, and modelling. *Sci Total Environ.* 2012
460 Nov 15;439:299-306.

461 Fukushi, K., Ishio, N., Urayama, H., Takeda, S., Wakida, S., Hiroy, K., 2000. Simultaneous
462 determination of bromide, nitrite and nitrate ions in seawater by capillary zone
463 electrophoresis using artificial seawater as the carrier solution. *Electrophoresis* 21, 388-395.

464 Gewert, B., Plassmann, M. M., MacLeod, M., 2015. Pathways for degradation of plastic polymers
465 floating in the marine environment. *Environ. Sci. Process. Impacts.* 17, 1513-1521.

466 Geyer, R., Jambeck, J. R., Law, K. L., 2017. Production, use, and fate of all plastics ever made. *Sci.*
467 *Adv.* 3, 1700782.

468 Gligorovski, S., Streckowski, R., Barbati, S., Vione, D., 2015. Environmental implications of
469 hydroxyl radicals ($\cdot\text{OH}$). *Chem. Rev.* 115, 13051-13092.

470 Guo, Z., Kodikara, D., Shofi Albi, L., Hatano, Y., Chen, G., Yoshimura, C., Wang, J., 2022.
471 Photodegradation of organic micropollutants in aquatic environment: Importance, factors and
472 processes. *Water Res.* 118236, in press.

473 Hug, G. L., 1981. Optical spectra of non-metallic inorganic transient species in aqueous solution.
474 NSRDS-NBS 69, US. Washington DC: Government Printing Office.

475 Jakubowicz, I., Enebro, J., Yarahmadi, N., 2021. Challenges in the search for nanoplastics in the
476 environment - A critical review from the polymer science perspective. *Polymer Testing* 93,
477 106953.

478 Jambeck, J. R., Geyer, R., Wilcox, C., Siegler, T. R., Perryman, M., Andrady, A., Narayan, R.,
479 Law, K. L., 2015. Marine pollution. Plastic waste inputs from land into the ocean. *Science*
480 347, 768-771.

481 Katagi, T., 2018. Direct photolysis mechanism of pesticides in water. *J. Pestic. Sci.* 43, 57-72.

482 Kumar, M., Xiong, X., He, M., Tsang, D. C. W., Gupta, J., Khan, E., Harrad, S., Hou, D., Ok, Y. S.,
483 Bolan, N. S., 2020. Microplastics as pollutants in agricultural soils. *Environ Pollut.* 265,
484 114980.

485 Liu, L., Xu, K., Zhang, B., Ye, Y., Zhang, Q., Jiang, W., 2021. Cellular internalization and release
486 of polystyrene microplastics and nanoplastics. *Sci. Total Environ.* 779, 146523.

487 Loiselle, S. A., Azza, N., Cozar, A., Bracchini, L., Tognazzi, A., Dattilo, A., Rossi, C., 2008.
488 Variability in factors causing light attenuation in Lake Victoria. *Freshwater Biology* 53, 535-
489 545.

490 McNeill, K., Canonica, S., 2016. Triplet state dissolved organic matter in aquatic photochemistry:
491 Reaction mechanisms, substrate scope, and photophysical properties. *Environ. Sci.: Processes*
492 *Impacts* 18, 1381-1399.

493 Neta, P., Huie, R. E., Ross, A. B., 1988. Rate constants for reactions of inorganic radicals in
494 aqueous solution. *J. Phys. Chem. Ref. Data* 17, 1027.

495 Ossola, R., Jönsson, O. M., Moor, K., McNeill, K., 2021. Singlet oxygen quantum yields in
496 environmental waters. *Chem.Rev.* 121, 4100-4146.

497 Parker, K. M., Mitch, W. A., 2016. Halogen radicals contribute to photooxidation in coastal and
498 estuarine waters. *Proc. Natl. Acad. Sci. USA* 113, 5868-5873.

499 Rosario-Ortiz, F. L., Canonica, S., 2016. Probe compounds to assess the photochemical activity of
500 dissolved organic matter. *Environ. Sci. Technol.* 50, 12532-12547.

501 Salthammer, T., 2022. Microplastics and their additives in the indoor environment. *Angew. Chem.*
502 *Int. Ed. Engl.* 61, e202205713.

503 Schmidt, C., Krauth, T., Wagner, S., 2017. Export of plastic debris by rivers into the sea. *Environ*
504 *Sci Technol.* 51, 12246-12253.

505 Silva, M. P., Mostafa, S., McKay, G., Rosario-Ortiz, F. L., Teixeira, A. C. S. C., 2015.
506 Photochemical fate of amicarbazono in aqueous media: Laboratory measurement and
507 simulations. *Environ. Engin. Sci.* 32, 730-740.

508 Silva, M. P., Acosta, A. M. L., Ishiki, H. M., Rossi, R. C., Mafra, R. C., Teixeira, A. C. S. C., 2019.
509 Environmental photochemical fate and UVC degradation of sodium levothyroxine in aqueous
510 medium. *Environ. Sci. Pollut. Res.* 26, 4393-4403.

511 US-EPA, 2021. Estimation Programs Interface Suite™ for Microsoft® Windows, v. 4.11. United
512 States Environmental Protection Agency, Washington, DC, USA.

513 Vione, D., Bagnus, D., Maurino, V., Minero, C., 2010. Quantification of singlet oxygen and
514 hydroxyl radicals upon UV irradiation of surface water. *Environ. Chem. Lett.* 8, 193–198.

515 Vione, D., Scozzaro, A., 2019. Photochemistry of surface fresh waters in the framework of climate
516 change. *Environ. Sci. Technol.* 53, 7945-7963.

517 Vione, D., 2020. A critical view of the application of the APEX software (Aqueous Photochemistry
518 of Environmentally-occurring Xenobiotics) to predict photoreaction kinetics in surface
519 freshwaters. *Molecules* 25, 9.

- 520 Wojnárovits, L., Tóth, T., Takács, E., 2020. Rate constants of carbonate radical anion reactions with
521 molecules of environmental interest in aqueous solution: A review. *Sci. Total Environ.* 717,
522 137219.
- 523 Wols, B. A, Hofman-Caris, C. H., 2012. Review of photochemical reaction constants of organic
524 micropollutants required for UV advanced oxidation processes in water. *Water Res.* 46,
525 2815-2827.
- 526 Yan, S., Song, W., 2014. Photo-transformation of pharmaceutically active compounds in the
527 aqueous environment: a review. *Environ. Sci.: Processes Impacts* 16, 697-720.
- 528 Yan, S., Liu, Y., Lian, L., Li, R., Ma, J., Zhou, H., Song, W., 2019. Photochemical formation of
529 carbonate radical and its reaction with dissolved organic matters. *Water Res.* 161, 288-296.
- 530 Zhu, L., Zhao, S., Bittar, T. B., Stubbins, A., Li, D., 2020. Photochemical dissolution of buoyant
531 microplastics to dissolved organic carbon: Rates and microbial impacts. *J. Hazard. Mater.*
532 383, 121065.



Click here to access/download
Supplementary Material
Bz-AcPh_SM.pdf

